

Evaluating Icing Nowcasts using CloudSat

Thomas F. Lee*, Cristian Mitrescu, Richard Bankert
Naval Research Laboratory, Monterey, California

Cory A. Wolff
National Center for Atmospheric Research, Boulder, Colorado

Steven D. Miller
Cooperative Institute for Research in the Atmosphere, Fort Collins, Colorado

(Manuscript received 17 November 2009; in final form 31 March 2010)

ABSTRACT

The Current Icing Product (CIP) is a model/observation fusion tool to diagnose aircraft icing probability and severity. Implemented at the Aviation Weather Center, it is used by forecasters to assess icing conditions and improve aviation support over the contiguous United States and southern Canada. However, given the three dimensional nature of the icing threat, it has been difficult to completely assess CIP effectiveness. CloudSat is a low-earth orbiting satellite containing a 3 mm cloud radar (94 GHz) that gives a two dimensional vertical profile of cloud along the orbital track of the satellite. When combined with temperature profile information, CloudSat can be used to infer information about the location and vertical structure of supercooled liquid water. Therefore, it can be used to compare to CIP. In this study first we compare CIP and CloudSat in several case studies to illustrate CIP's strengths and limitations. In the process we illustrate that CloudSat products are powerful observational tools in their own right, allowing unprecedented cross-sectional views of cloud systems which contain aviation hazards. Second, we compare CloudSat and CIP cloud heights statistically. For low cloud systems in particular, CIP tends to analyze cloud tops that are too high, leading to vertical overestimation of the icing hazard.

* *Corresponding author address*: Thomas F. Lee, Naval Research Laboratory, 7 Grace Hopper Avenue, Monterey, CA, 93943-5502. E-mail: Thomas.lee@nrlmry.navy.mil

1. Introduction

CloudSat flies in the ‘A-Train’ constellation at 1330 local time ascending node (Stephens et al. 2002). While it does not detect cloud phase, a factor in aircraft icing studies, it does give a detailed depiction of cloud vertical structure. Moreover, when combined with vertical temperature profiles from a numerical model, CloudSat can supply important clues about the location of supercooled liquid water (SLW). Launched on April 28, 2006, CloudSat is a NASA Earth observation satellite that uses radar to measure the altitude and properties of clouds. The instrument on CloudSat is the Cloud Profiling Radar (CPR), a 94-GHz nadir-looking instrument that measures both the returned backscattered energy by clouds as well as cloud location and altitude. CloudSat has been validated over cold season cloud systems in the context of the Canadian Calipso Validation Project using instruments from coincident aircraft overpasses (Hudak et al. 2006).

CloudSat has a 240 m vertical range resolution between the surface and 30 km. Due to surface contamination from ground clutter, the usefulness of cloud information is limited below 1.5 km. CloudSat observes a single row of pixels along its flight path with footprint size of 1.4 x 3.5 km. Although CloudSat is not routinely used in forecast offices, the Naval Research Laboratory (NRL) posts products several hours after overpass time (Miller et al. 2006; <http://www.nrlmry.navy.mil/NEXSAT.html>). The utility of these active sensors for validating the Current Icing Product (CIP), an aircraft icing nowcast, is demonstrated in several case studies.

2. Current Icing Product (CIP) and other Icing Algorithms

The CIP algorithm (Bernstein et al. 2005) combines satellite, radar, surface, lightning, and pilot-report observations (PIREPs) with model output to create a detailed three-dimensional hourly diagnosis of the potential for icing and supercooled large drops along with icing severity. These inputs are merged using decision-tree and fuzzy logic. CIP was developed as a tool for diagnosing in-flight icing conditions from the surface to 30,000 ft MSL over the continental United States and southern Canada at 20 km horizontal resolution. CIP is available from the NOAA Aviation Weather Center: <http://adds.aviationweather.gov/icing/>.

Cloud physics principles, along with field program results, form the basis for the final products. CIP tends to overestimate cloud tops, especially at low altitudes, resulting in a greater volume of potentially icing-impacted airspace than in reality. Validation of CIP has been difficult in the past because of a lack of observational truth data. Pilots seldom report cloud tops and bases and information on cloud layers, and therefore reports are often not optimal for validation. A three dimensional analysis of clouds is the first step in the approach by CIP to analyze regions of likely icing in near real time. In the CIP scheme satellite and surface data are used to reduce the vertical and areal extent of cloud fields predicted by numerical model estimates (Schultz and Politovich 1992). This filtering leads to a reduction of the area warned in subsequent icing nowcasts (Thompson et al. 1997). Satellite screening, using passive infrared and visible techniques, often fails to eliminate many clouds. For example, cirrus obscures information about clouds in the lower troposphere. CloudSat however is capable of detecting clouds throughout the vertical column and therefore can operate as an important check to the effectiveness of CIP.

CIP currently uses a combination of satellite and model data to identify the cloud top. In cloudy areas the cloud top height (CTZ) algorithm compares the temperature measured at the top

of the cloud by the infrared channel to a model sounding of temperatures, starting at the top. Because the horizontal resolution of CIP is 20 km and the satellite data from GOES is 5 km horizontal resolution, there are up to 16 pixels of satellite data for every CIP point. The infrared temperatures from the cloudy pixels are sorted and the 90th percentile coldest is used as the cloud top temperature for the entire CIP grid point. The cloud top height is then set to one model level above where the model temperature first becomes warmer than the cloud top temperature (Bernstein et al. 2005).

3. Case Examples

Fig. 1 shows visible satellite imagery associated with an icing event over New York state and southern Canada. The CIP map (Fig. 2) indicates moderate icing over this region between the surface and up to 5 km (~16000 ft). The CloudSat trace (Fig. 2) shows that the icing layer is very shallow, around 2-3 km above ground level, just deep enough to be detectable by CloudSat. The CIP trace shows much deeper icing at about 4-5 km above ground level, which based on comparison with CloudSat, is too high. This case study represents an occasional tendency for CIP to overestimate the cloud tops of low cloud systems.

Fig. 3 shows an icing event extending from the Mid-Atlantic States into Canada. The CIP (top diagram Fig. 4) depicts heavy icing severity to the north and a lesser severity in Pennsylvania and Virginia (Fig. 4). Comparison of the CIP cross section with the CloudSat trace shows good agreement in the northern regions (right end of trace) but reveals a discrepancy over the Mid-Atlantic states (“Icing Layer Aloft”). CIP suggests an icing layer aloft while CloudSat shows little or no cloud. Research is continuing to determine whether this type of discrepancy, which occurs from time to time, is due to a problem in CIP, in CloudSat or in both. It may be that CloudSat could fail to detect very thin clouds that are depicted by CIP.

The Geocolor satellite picture in Fig. 5 shows thick overcast over the Central Plains with the CloudSat trace transecting the country. The icing outbreak has multiple confirmations over Kansas and Missouri (Fig. 6), indicated by the presence of icing PIREPs. The CIP trace barely hints at icing in two major icing layers, a layer at about 2-3 km, and a higher one at about 6-7 km. CloudSat confirms this double layer. Cloud layers can often go undetected in CIP, which relies solely on model data for layer detection.

The CIP maximum icing severity map view (Fig. 7) depicts an icing event in northern California. The CloudSat trace (middle diagram) shows the associated deep cloud system in profile over the Sierra Nevada mountain range. The cloud pattern, which contains several examples of pilot reports of icing, matches well with the CIP profile (bottom diagram). Note that the icing layer shown by CIP (with tops at about 5 km) is lower than the echo shown by CloudSat. This is because icing in CIP is generally limited to layers below about the -25°C level.

In contrast to Fig. 7, which depicted a deep icing layer over a mountain range, the case in Figs. 8 and 9 illustrates a very shallow cloud system at mountain top in California and Nevada. The CloudSat trace illustrates that the cloud system is limited to the higher terrain of the Sierra Nevada and surrounding ranges. The CIP trace reveals a similar pattern.

Fig. 10 shows a Geocolor product of a mostly shallow cloud system centered over Indiana. The CIP graphic (Fig. 11, top map) indicates light icing severity (integrated through the column) in blue and shows numerous PIREPs indicating icing over this region. CloudSat does not show any clouds here, but icing PIREPs confirm the presence of clouds and icing in the vicinity. In addition, the CIP cross section (Fig. 11 bottom diagram) shows an icing layer in this vicinity which corresponds to the location of the PIREPs. The explanation for the lack of a CloudSat cloud signature is that due to ground clutter, the instrument can not detect clouds lower

than 1.5 km. Although the capacity to use CloudSat as a validation tool is limited in this case, it still informs us that the CIP icing top, at about 3 km, is possibly in error, though there is a positive icing PIREP around 3 km.

4. Validation

We assumed that the nearly exact measurement of many low and midlevel clouds from CloudSat could help validate the current CIP and lead to improvements. However, CloudSat and CIP did not always agree on the presence or absence of a cloud. 73% of the grid points where CloudSat observed a cloud also contained a CIP cloud. Reasons for the discrepancies include, but are not limited to, bad or missing satellite data in CIP, high, thin cirrus that were observed by CloudSat but not CIP, and time discrepancy issues such as CIP clouds moving or dissipating before/after the CPR pass. Additionally, there were instances in which CloudSat was blocked from seeing the lowest cloud tops containing icing (below 1.5 km) because of ground clutter. This section will focus on the 38,000+ grid points where both datasets agreed on the existence of a cloud.

Because the spatial and temporal resolutions of the datasets are quite different some smoothing was necessary. First, the datasets needed to be matched in time. CIP is run hourly, while the CloudSat CPR measures reflectivity every 0.16 s (Stephens et al. 2002). For this study all of the CloudSat measurements within a half hour of the CIP valid time were matched to the CIP CTZ. For example, CloudSat data between 1730 and 1830 UTC were matched to CIP CTZ output with a valid time of 1800 UTC.

The fast sampling rate of CloudSat results in many measurements which occur in the same CIP grid point (20 km horizontal resolution). To find good matches between the datasets

we counted the total number of observations from CloudSat within each CIP grid point. If at least 75% of those observations contained a valid cloud, then that grid point was considered to be cloudy. This reduced the amount of broken clouds in the dataset, which CIP would not be able to diagnose with its coarser resolution. The median CTZ from the CloudSat measurements was then compared to the corresponding CIP CTZ for that grid point. This was done for all CloudSat passes over the CIP domain between January and March 2007, resulting in 38,000 matches.

The median difference in CTZ was -108 m, which means that, statistically, the CIP CTZ was 108 m *lower* than the CloudSat measured value. This difference is close to the CloudSat vertical resolution of ± 240 m (± 1 range gate). Importantly, however, the median difference, while representative of the entire dataset, varies with the cloud top height. Fig. 12 shows the difference distributions for cloud top heights (from CloudSat) less than 3 km, 3-6 km, 6-9 km, and greater than 9 km. The median difference for each of these bins is also indicated. For the lowest clouds 85% of the differences are greater than 240 m (light blue bars), meaning that CIP tends to over-diagnose the tops of these clouds. For higher cloud tops CIP underestimates CTZ. For cloud tops above 9 km 70% of the differences are less than -240 m (red bars). The median difference also reflects this trend for each altitude level, going from 1469 m for the low clouds to -592 m for the highest ones. The upper mid-level clouds (6 – 9 km) have the lowest median difference (-27 m) but the high clouds (9+ km) have the highest percentage of points between -240 and 240 m (17%; green bars).

Fig. 13 gives an alternative visualization. The first (left hand side) is for all clouds, then for clouds less than 3 km, 3 – 6 km, 6 – 9 km, and above 9 km. The median is represented by the bold dash in the middle with the shaded regions extending to the 25th and 75th percentiles. The whiskers extend to the 5th and 95th percentiles. The figure suggests that nearly all of the cloud

tops in CIP are an overestimate for low level clouds. Consistent with Fig. 12, all values (from 0 – 3 km toward the right) decrease with increasing cloud top height, suggesting increasing underestimates by CIP. The most spread is seen in the 9+ km clouds.

5. Discussion & Future Work

CloudSat gives unprecedented views of cloud structure that can be used to better understand icing environments. Infrared and visible satellite images are capable of detecting cloud tops, but observation of low-level structure is often blocked by higher layers. While weather radars have shown forecasters precipitation structure for years in the vicinity of icing events, the associated cloud structure has been missed. CloudSat enables direct observation of the clouds which are often responsible for icing events. However, CloudSat and CIP output must be compared with caution since CIP output is strongly constrained in the vertical by temperature (0 to -25°C levels), and also limited by its much coarser horizontal and vertical resolution.

Compared to CloudSat validation, CIP appears to have cloud tops that are too high for low altitude clouds and too low for high altitude clouds. The over-estimates at low altitudes are expected. Comparisons with research aircraft data have shown that CIP often overestimates the cloud top height when a strong inversion is present, which is common in low-level wintertime clouds (e.g., a post-cold frontal stratus layer). The inversion is too weak often in the model used as a vertical temperature benchmark, which results in a CTZ that is too high, since the satellite observed cloud top temperature (CTT) matches the model temperature sounding well above the base of the inversion. This adds icing volume to CIP and decreases its efficiency.

The lower CIP cloud tops at higher altitudes, on average, decreases cloud volume in CIP, but does not result in a decrease in the icing volume, mostly because CIP does not diagnose icing

near the tops of these higher clouds. The minimum temperature for icing in CIP is -25°C except in convection where the minimum temperature threshold decreases to -30°C . Therefore, this effect is quite small and is likely due to anomalously warm infrared temperatures caused by transparent cirrus. This leads to CIP cloud tops which are too low in comparison to CloudSat.

A new CTZ algorithm has recently been developed for CIP that seeks to improve the cloud top height diagnosis by combining satellite data with other model fields such as equivalent potential temperature, condensate, relative humidity, and vertical velocity. This new method has been shown to reduce excessive icing volume without sacrificing CIP's skill at detecting actual icing. The new CIP CTZ method is currently being run internally, and the CloudSat data will be used to gauge its accuracy and determine if it decreases (increases) the diagnosed CTZ at low (high) altitudes. The CTZ algorithm in the Forecast Icing Product (FIP) will undergo a similar validation.

Acknowledgments

The support of our research sponsor, the Office of Naval Research under program element number PE-0602435N is gratefully acknowledged. This research is in response to requirements and funding by the Federal Aviation Administration (FAA). The views expressed here are those of the authors and do not necessarily represent the official policy or position of the FAA.

REFERENCES

- Bernstein, B. C., F. McDonough, M. P. Politovich, B. G. Brown, T. P. Ratvasky, D. R. Miller, C. A. Wolff, and G. C. Cuning, 2005: Current Icing Potential (CIP): Algorithm description and comparison with aircraft observations. *J. Applied Met.*, **44**, 969 – 986.
- Hudak, D., H. Barker, P. Rodriguez, and D. Donovan, 2006: The Canadian CloudSat Validation Project. 4th European Conf. on Radar in Hydrology and Meteorology, Barcelona, Spain, 18-22 Sept., 2006, 609-612.
- Miller, S. D., J. D. Hawkins, J. Kent, F. J. Turk, T. F. Lee, A. P. Kuciauskas, K. Richardson, R. Wade, and C. Hoffman, 2006: NEXSAT: Previewing NPOESS/VIIRS Imagery Capabilities. *Bull. Amer. Meteor. Soc.*, **87**, 433-446.
- Schultz, P. and M. K. Politovich, 1992: Toward the improvement of aircraft-icing forecasts for the continental United States, *Wea. Forecasting*, **7**, 491–500.
- Stephens, G. L., et al, 2002: The CLOUDSAT Mission and the A-Train, *Bull. Amer. Met. Soc.*, **83**, 1771-1790.
- Thompson, G., R. Bullock, and T. F. Lee, 1997: Using satellite data to reduce spatial extent of diagnosed icing. *Wea. Forecasting*, **12**, 185–190.

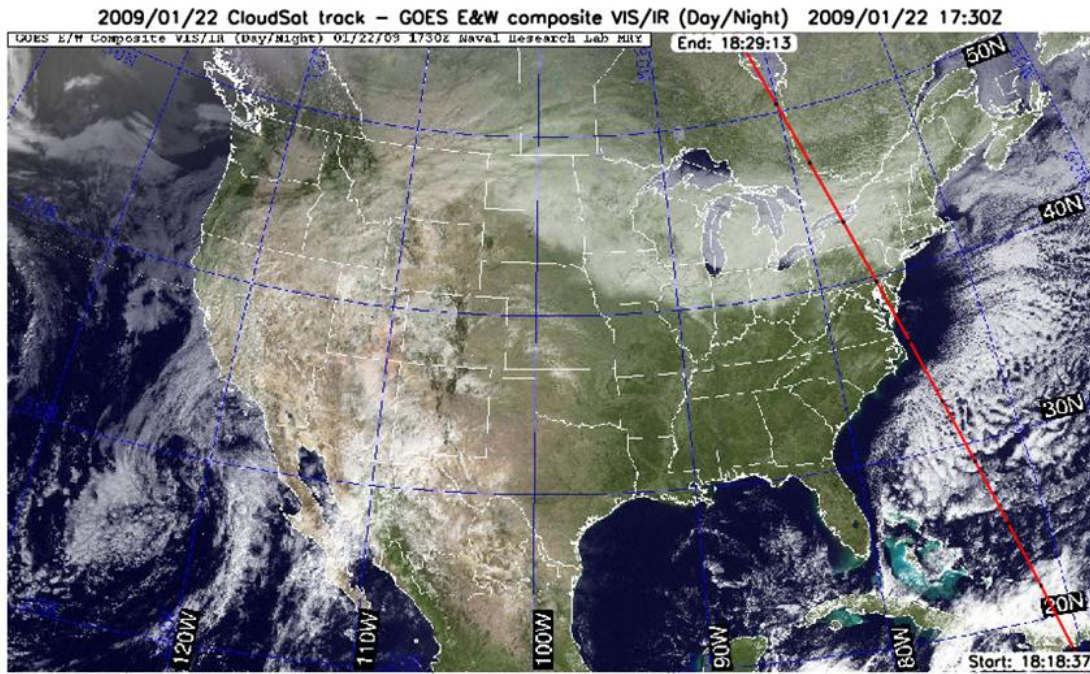


Figure 1. Geocolor GOES Visible/IR Composite, 22 January 2009. Red line indicates position of cross sections in Fig. 2.

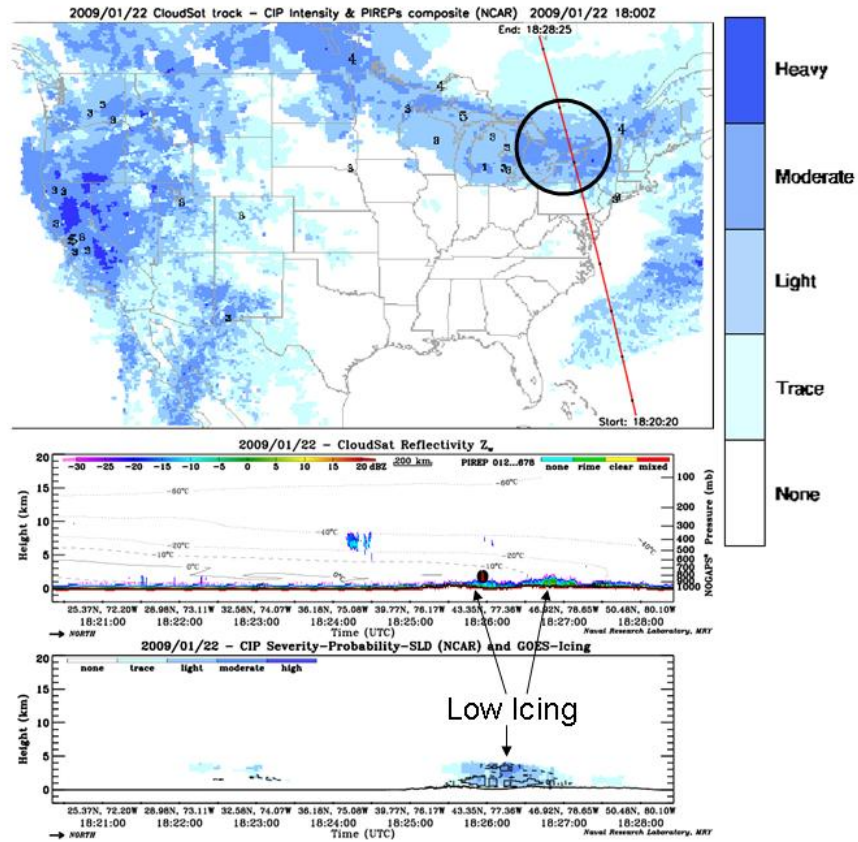


Figure 2. Upper Diagram: CIP Maximum Icing Severity Map; Middle Diagram: CloudSat Depiction with PIREPs; Lower Diagram: CIP Cross Section. Date same as Figure 1.

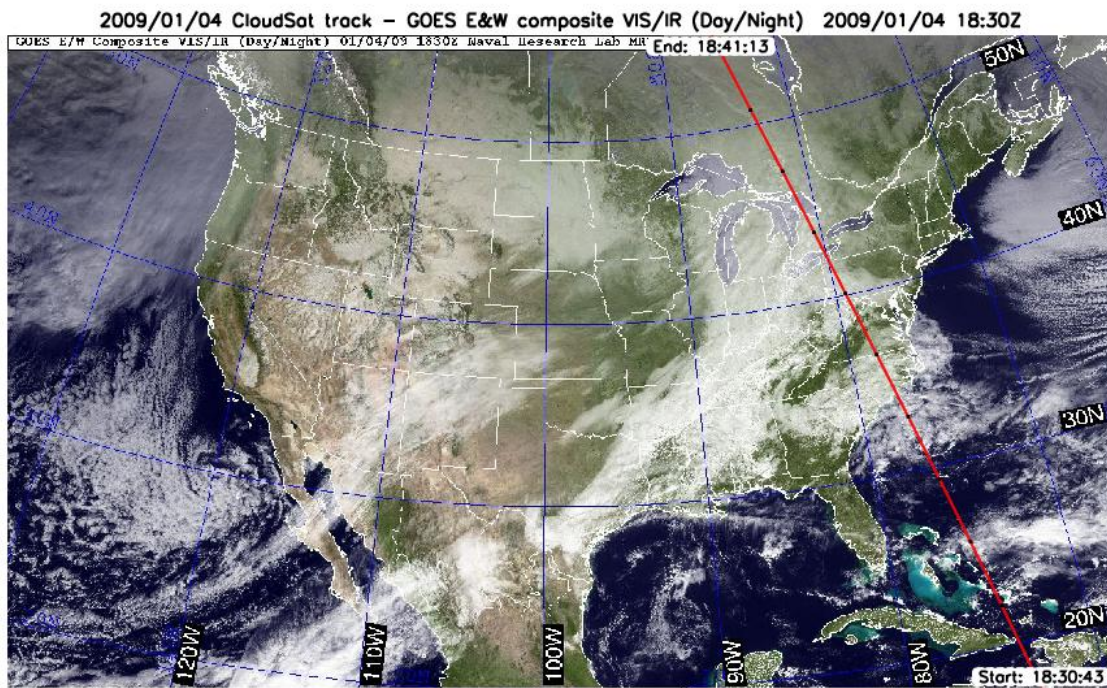


Figure 3. Geocolor GOES Visible/IR Composite, 4 February 2009. Red line indicates position of cross sections in Fig. 4.

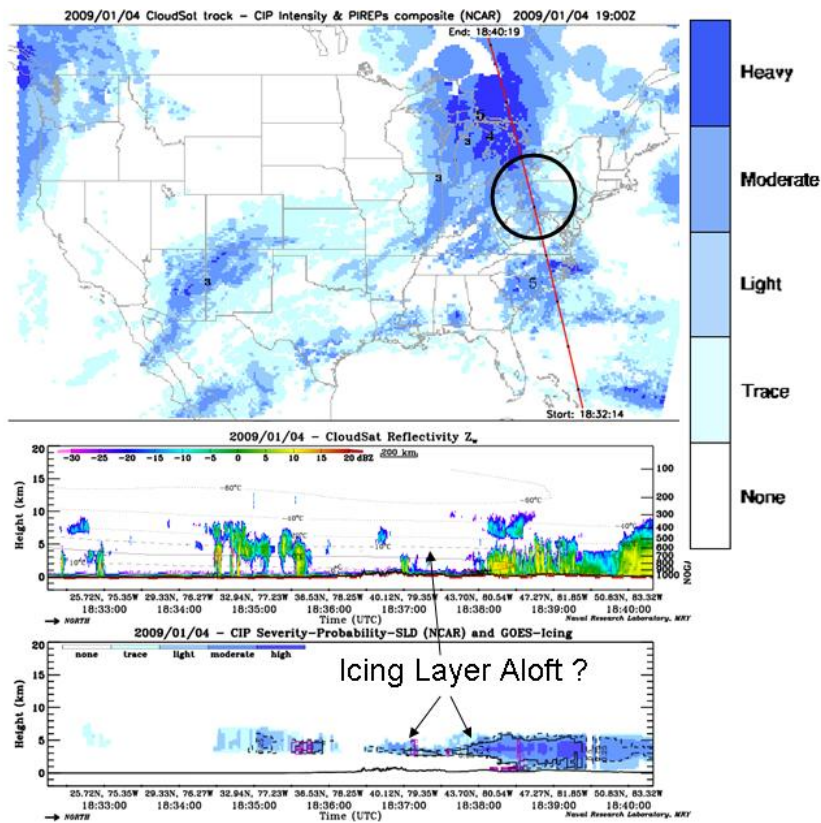


Figure 4. Upper Diagram: CIP Maximum Icing Severity Map; Middle Diagram: CloudSat Depiction with PIREPs; Lower Diagram: CIP Cross Section. Date same as Figure 3.

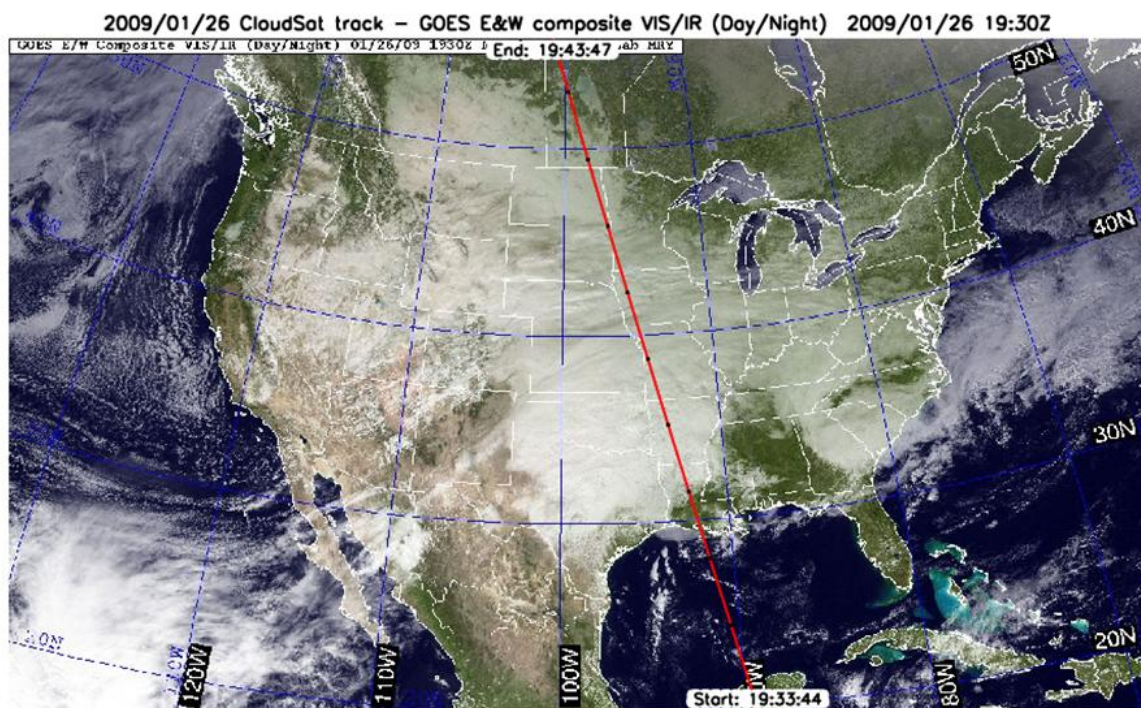


Figure 5. Geocolor GOES Visible/IR Composite, 26 January 2009. Red line indicates position of cross sections in Fig. 6.

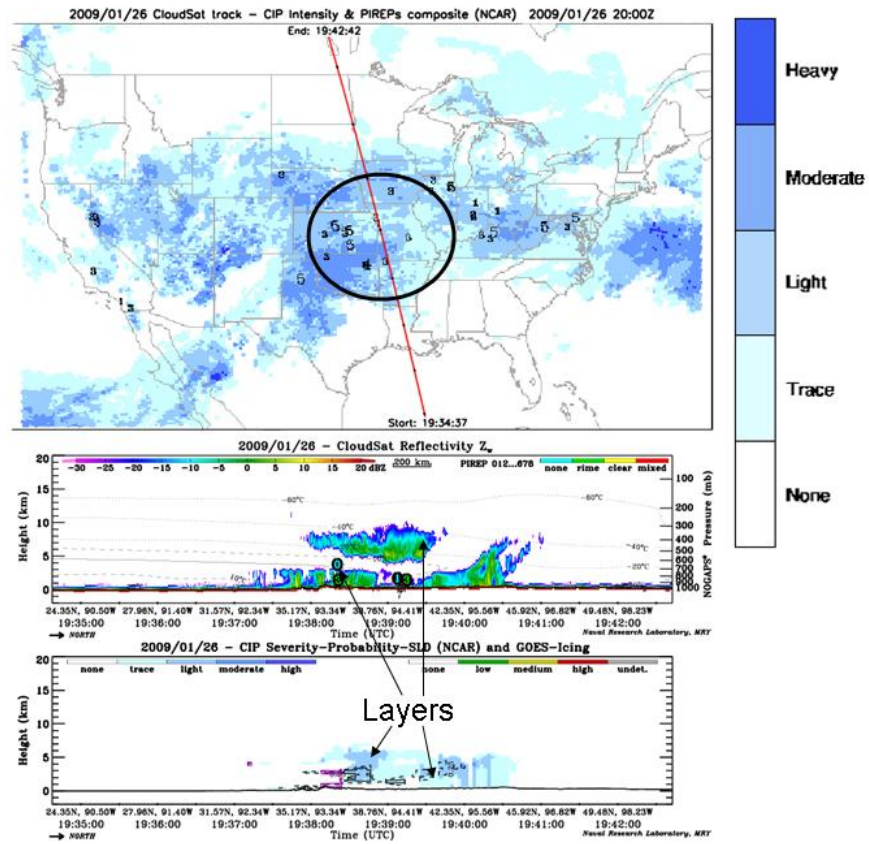


Figure 6. Upper Diagram: CIP Maximum Icing Severity Map; Middle Diagram: CloudSat Depiction with PIREPs; Lower Diagram: CIP Cross Section. Date same as Figure 5.

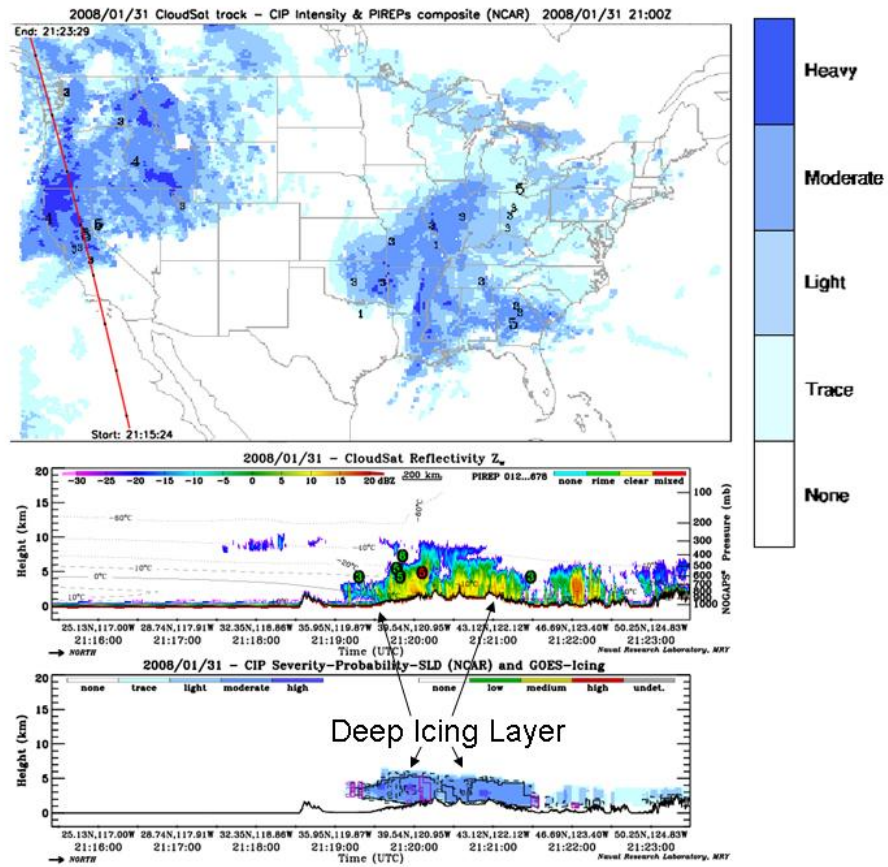


Figure 7. Upper Diagram: CIP Maximum Icing Severity Map; Middle Diagram: CloudSat Depiction with PIREPs; Lower Diagram: CIP Cross Section. 31 January 2008.

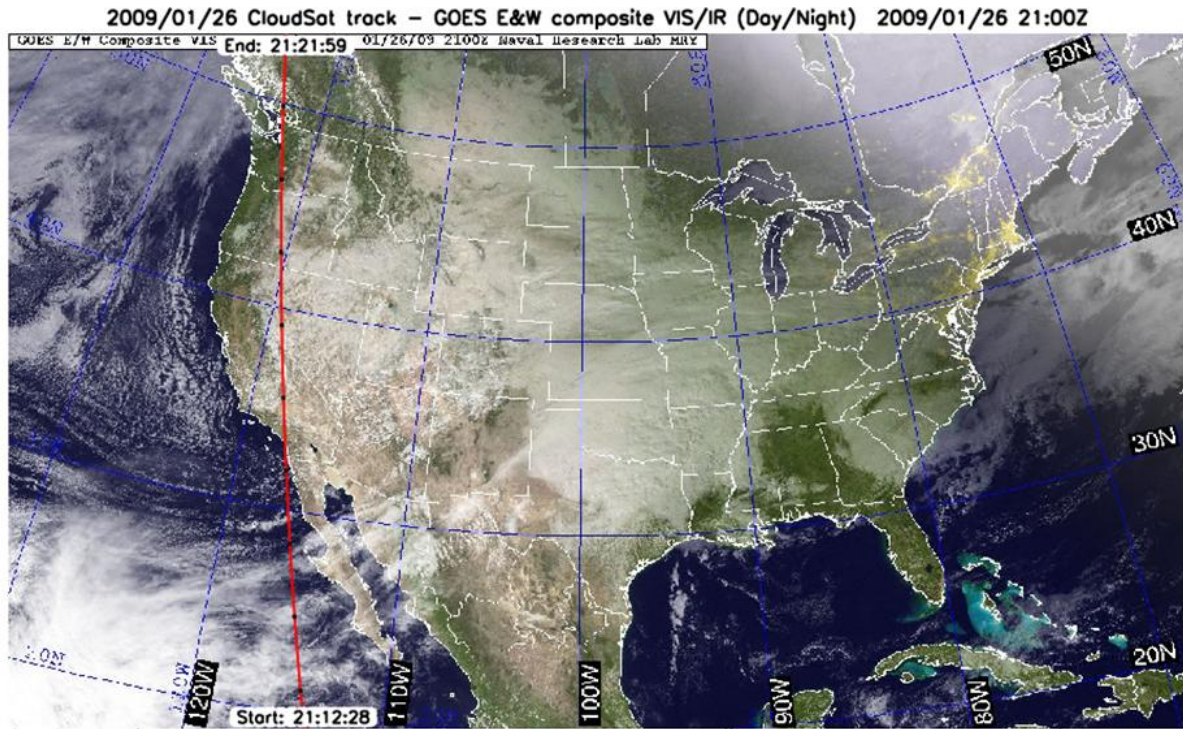


Figure 8. Geocolor GOES Visible/IR Composite, 26 January 2009. Red line indicates position of cross sections in Fig. 9.

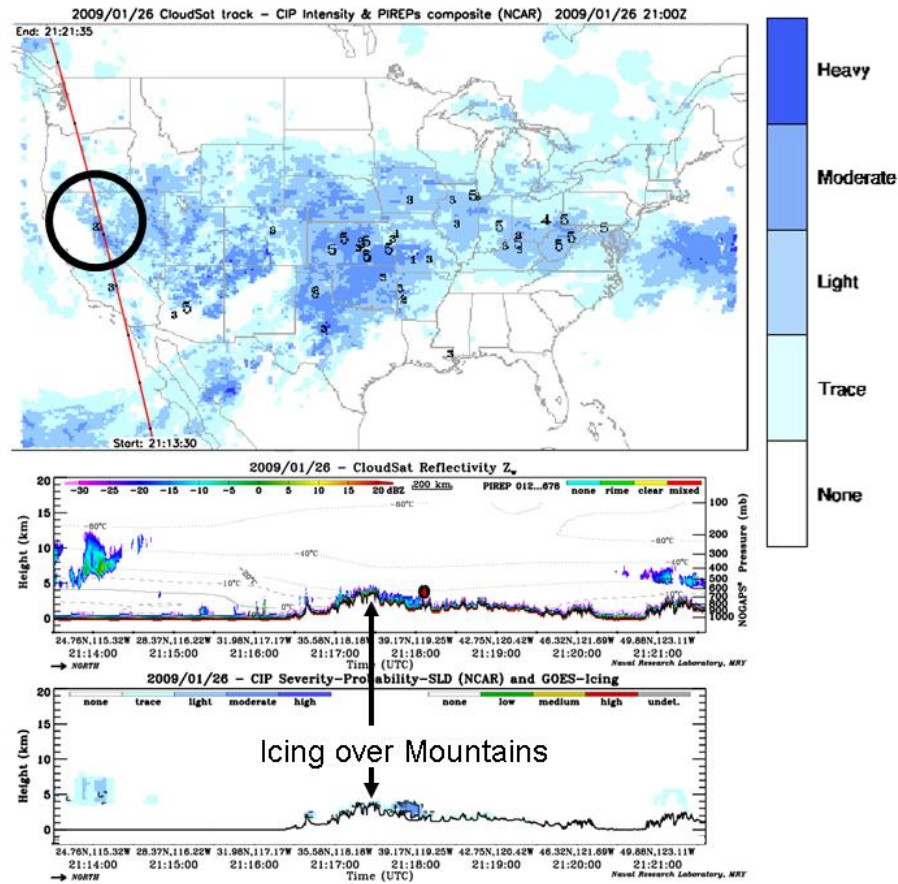


Figure 9. Upper Diagram: CIP Maximum Icing Severity Map; Middle Diagram: CloudSat Depiction with PIREPs; Lower Diagram: CIP Cross Section. Date same as Figure 8.

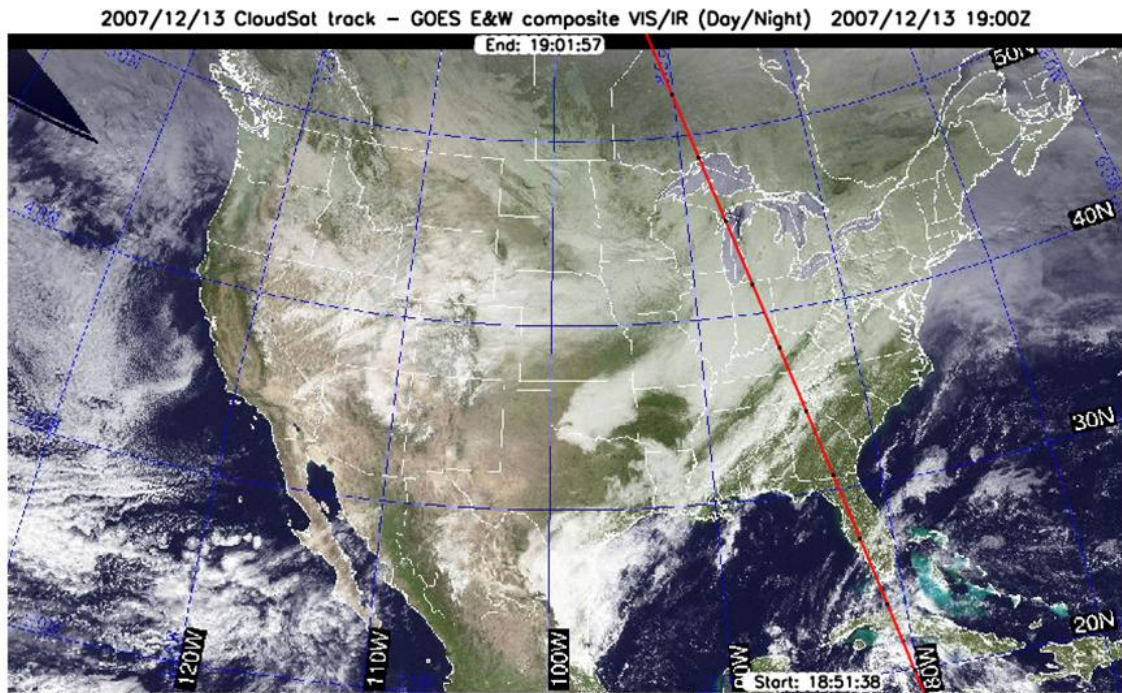


Figure 10. Geocolor GOES Visible/IR Composite, 13 December 2007. Red line indicates position of cross sections in Fig. 11.

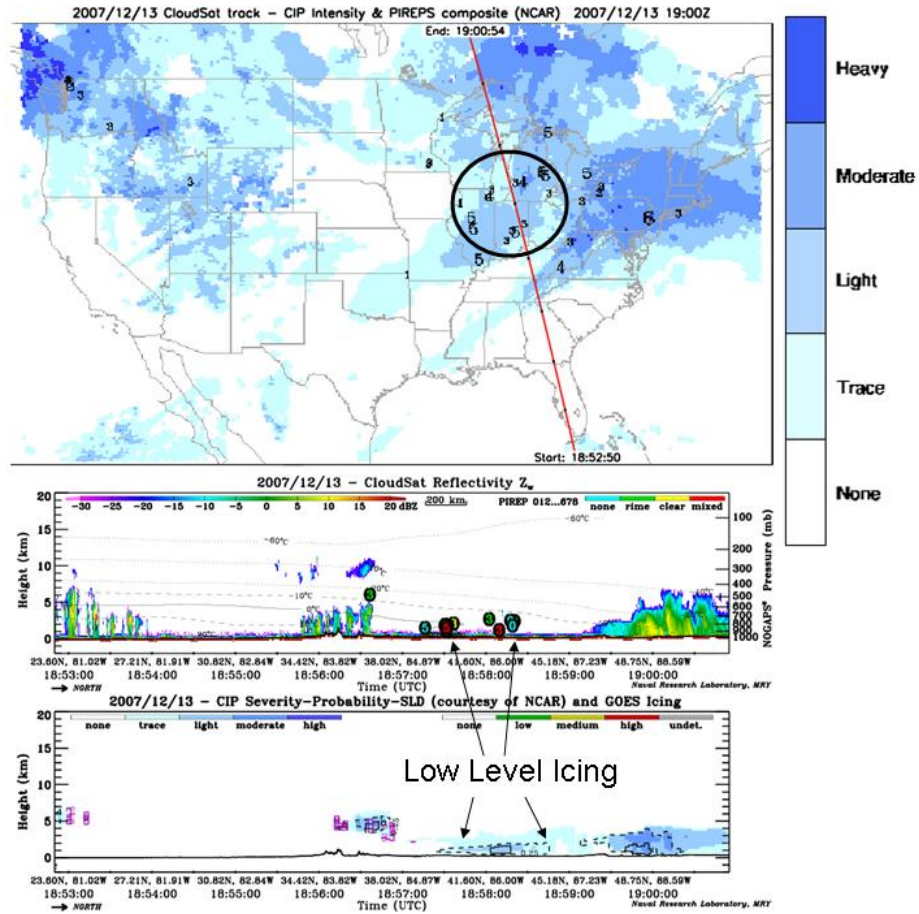


Figure 11. Upper Diagram: CIP Maximum Icing Severity Map; Middle Diagram: CloudSat Depiction with PIREPs; Lower Diagram: CIP Cross Section. Date same as Figure 10.

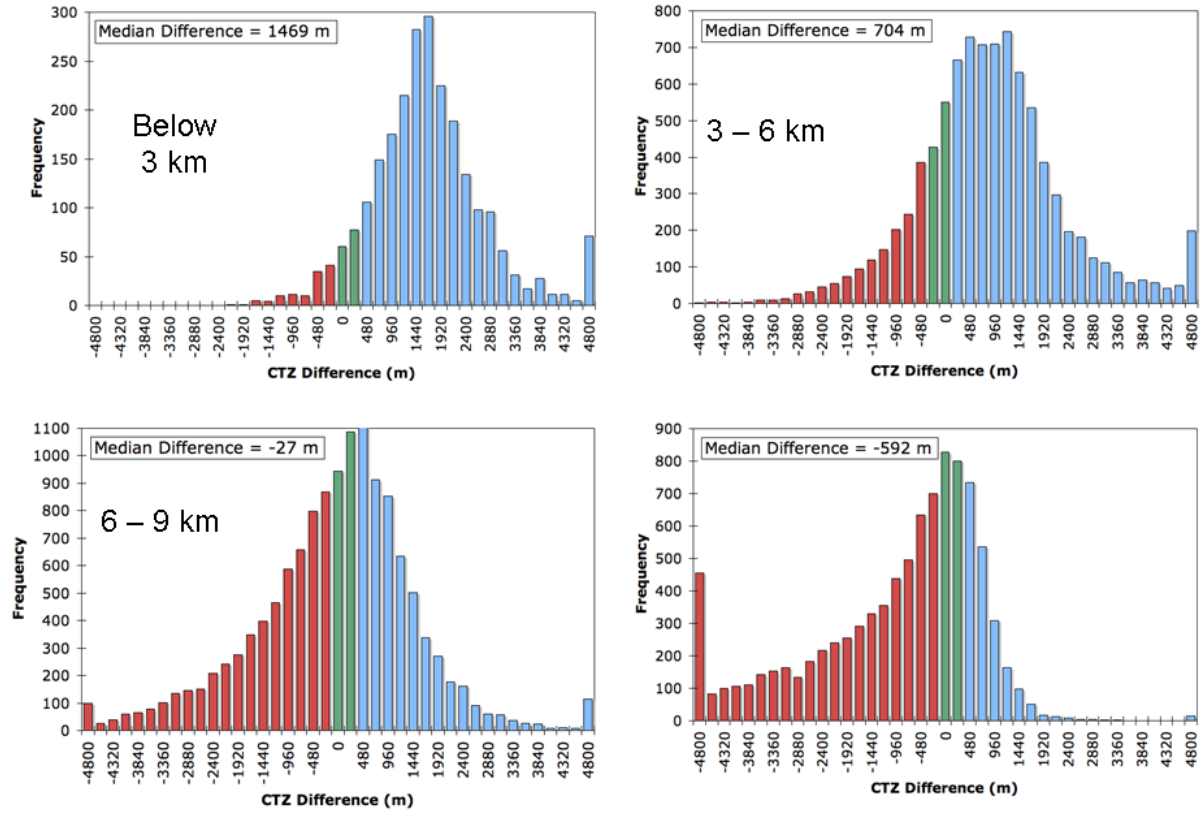


Figure 12. Distribution of differences between CIP and CloudSat CTZ observations (m) for CloudSat measured cloud tops with heights (a) < 3 km, (b) 3-6 km, (c) 6-9 km, (d) > 9 km. Red bars represent differences less than -240 m, green bars represent differences between -240 and 240 m, and blue bars represent differences greater than 240 m. The median differences for each bin are in the upper left corner.

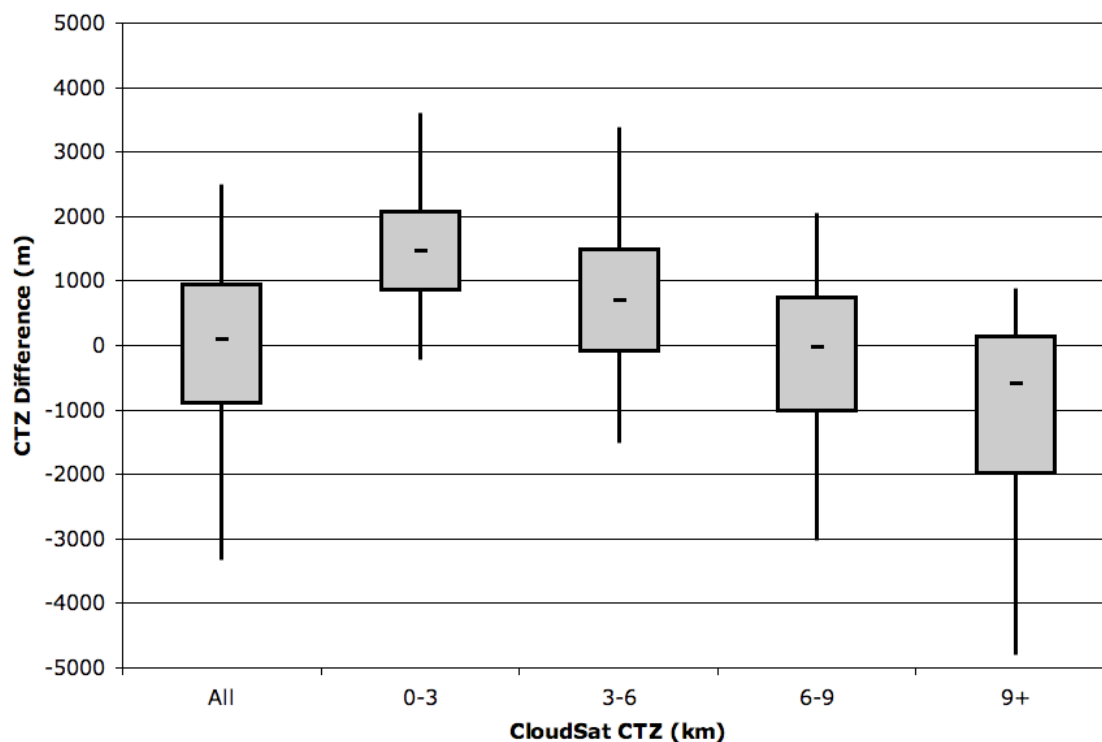


Figure 13. Box-and-whiskers diagram showing distributions of differences between CIP and CloudSat CTZ observations (m) for CloudSat measured cloud tops for all clouds, < 3 km, 3-6 km, 6-9 km, > 9 km. The median is represented by the bold dash in the middle with the shaded regions extending to the 25th and 75th percentiles. The whiskers extend to the 5th and 95th percentiles.